Accepted Manuscript

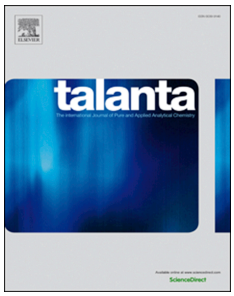

Co_3O_4 nanoparticles supported mesoporous carbon framework interface for glucose biosensing

Dhanjai, Putrakumar Balla, Ankita Sinha, Lingxia Wu, Xianbo Lu, Dongqin Tan, Jiping Chen

PII: S0039-9140(19)30539-9

DOI: https://doi.org/10.1016/j.talanta.2019.05.056

Reference: TAL 19941

To appear in: *Talanta*

Received Date: 8 February 2019

Revised Date: 4 May 2019

Accepted Date: 12 May 2019

Please cite this article as: Dhanjai, P. Balla, A. Sinha, L. Wu, X. Lu, D. Tan, J. Chen, Co_3O_4 nanoparticles supported mesoporous carbon framework interface for glucose biosensing, *Talanta* (2019), doi: https://doi.org/10.1016/j.talanta.2019.05.056.

This is a PDF file of an unedited manuscript that has been accepted for publication. As a service to our customers we are providing this early version of the manuscript. The manuscript will undergo copyediting, typesetting, and review of the resulting proof before it is published in its final form. Please note that during the production process errors may be discovered which could affect the content, and all legal disclaimers that apply to the journal pertain.

Grabhical Abstract

Advanced functional nanostructure based on cobalt oxide supported mesoporous carbon framework (Co_3O_4@MCF) has been synthesized and successfully applied for bioelectrochemical sensing of glucose.

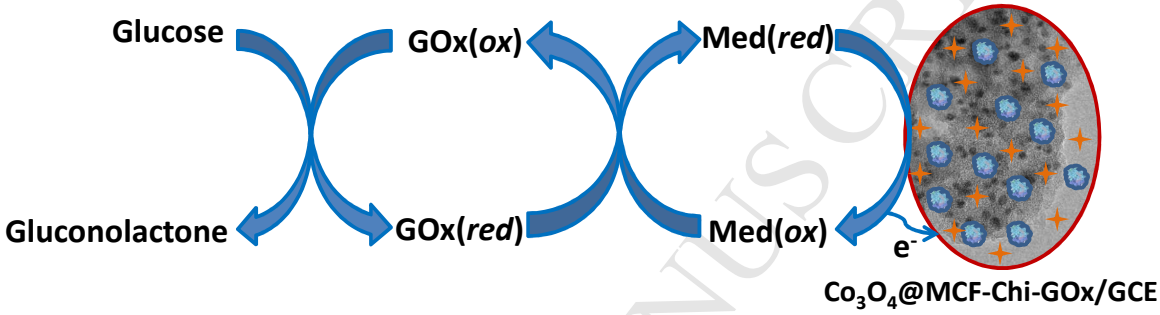

ACCEPTED MANUSCRIPT

ACCEPTED MANUSCRIPT

Co_3O_4 Nanoparticles Supported Mesoporous Carbon Framework Interface for Glucose Biosensing

Dhanjai[a], Putrakumar Balla[b], Ankita Sinha[c], Lingxia Wu[a], Xianbo Lu[a**], Dongqin Tan[a], Jiping Chen[a]*

[a]*CAS Key Laboratory of Separation Science for Analytical Chemistry, Dalian Institute of Chemical Physics, Chinese Academy of Sciences, Dalian 116023, China (dhanjai83@gmail.com).*

[b]*State Key Laboratory of Catalysis, Dalian Institute of Chemical Physics, Chinese Academy of Sciences, Dalian 116023, China.*

[c]*Key Laboratory of Industrial Ecology and Environmental Engineering (Ministry of Education, China), School of Environmental Science and Technology, Dalian University of Technology, Dalian-116024, PR China.*

**Corresponding E-mail: chenjp@dicp.ac.cn, xianbolu@dicp.ac.cn*

Abstract

The present work reports the preparation of advanced functional nanostructures based on cobalt oxide supported mesoporous carbon framework (Co_3O_4@MCF) for electrochemical biosensing. Co_3O_4@MCF was synthesized by simple hythrothermal & pyrolysis method and further characterized by various microscopic and spectroscopic techniques. The transmission electron microscopic (TEM) images show the lattice fringes of crystalline Co_3O_4 with interlayer spacing of 0.24 nm. The characteristic 311 plane in X-ray diffraction (XRD) studies further confirmed the presence of crystalline Co_3O_4 in carbon frameworks. Reflection of prominent A1g peak along with D and G band in raman spectra confirmed the successful fabrication of Co_3O_4@MCF nanocomposite. Prepared Co_3O_4@MCF manifested great porosity, good biocompatibility and large surface area which allowed effective immobilization of glucose oxidase (GOx) onto its surface using chitosan (Chi) as a binder. Thus, a nanocomposite (Co_3O_4@MCF-Chi-GOx) modified glassy carbon electrode (GCE) was fabricated for highly selective detection of glucose using amperometry and cyclic voltammetry. The Co_3O_4@MCF-

Chi-GOx/GCE electrode exhibited excellent biosensing performance for glucose monitoring with detection limit of (LOD) of 107.70 µM and reproducibility of 4.7 % RSD. Moreover, the biosensor holds great promise for its effective implications in point-of-care diagnostics of small biomolecules.

Keywords: Cobalt oxide supported mesoporous carbon framework (Co_3O_4@MCF), Glucose, Biosensors, Amperometry, Glucose oxidase.

ACCEPTED MANUSCRIPT

1. Introduction

Glucose (Glu) is one the most common metabolites of human body whose regulation is highly essential to avoid the risks of several diseases. For example, diabetes mellitus is a worldwide severe health problem which is caused by insulin deficiency and is generally reflected by glucose concentrations in blood. Normal glucose concentration in blood ranges from 4−7 mM whose alteration often causes adverse health impacts and lead to other severe metabolic disorders [1]. Therefore, an increasing demand for glucose sensors has been generated for onsite detection of blood glucose with high sensitivity, selectivity and stability. In recent times, electrochemical techniques have been proved to be reliable, fast and convenient approaches for sensing and biosensing applications [2-4]. So far, tremendous research efforts have been made to develop various electrochemical biosensing platforms for Glu monitoring [5]. Various electrochemical glucose sensors have been designed using conducting electrode surface of different nanomaterials [5, 6]. Furthermore, different biosensors based on the catalytic activities of biological receptors such as enzymes [7], whole cells [8], proteins [9] etc. have also been reported for glucose detection [5]. Glucose oxidase (GOx) has been considered as an ideal redox active enzymatic receptor and applied extensively to fabricate highly selective glucose biosensors [5]. However, direct electron transfer (DET) between the redox centers of GOx and electrode interfaces is highly complicated due to the complex structure of GOx scaffold. The redox active flavin adenine dinucleotide (FAD) of GOx is deeply protected from prosthetic protein shells. Therefore, realization of DET at conventional electrodes is very difficult [5, 10]. Over the past decades, various strategies have been applied to improve the catalytic activity of enzyme and to promote electron transfer between the redox centers of GOx and electrode surfaces. Nanomaterials with high electrical conductivity, large specific surface area and

excellent catalytic activity have been frequently utilized as supporting materials for immobilizing GOx onto the electrode surface to achieve improved electron transfer. Therefore, choice of a suitable electrode matrix is highly important. The immobilization should be done in such a way that the active site of enzyme stays in the close proximity of electrode surface to maintain the mechanical stability and catalytic activity of GOx [5, 10]. In past few years, a wide variety of electrode materials including carbon nanomaterials [11-20], metal nanoparticles [14-17, 21], metal oxides [22, 23], metal sulfides [19, 24], conducting polymers [17, 18, 20, 25] and ionic liquids [26] have been successfully applied to study electron transfer process of GOx. Consequently, a number of potential approaches have been reported for detection of Glu based on GOx nanocomposites.

Fabrication of biosensors has been highly challenging as miniaturization of electrodes to desired signal-to-noise ratio is an important aspect in electroanalysis. In recent times, rapid development in material sciences has offered new horizons for the synthesis of advance nanomaterials and their application in sensor fabrication and bioelectrochemical analysis. Mesoporous carbon (MC) is a novel kind of three dimensional nanostructured porous carbonaceous materials which has attracted a lot of attention for scientific applications [27-31] along with electrochemical purposes [32]. MC possesses various attractive features such as high biocompatibility, excellent electronic conductivity, high chemical inertness, wider electrochemical window, great porosity, large specific surface area, large pore volume and pore sizes which make it a suitable host matrix for immobilization of GOx at its surface [32-34]. Various modification schemes have been followed to prepare chemically functionalized MC nanocomposites to extend their scope in electrochemical sensing [33, 35]. Till date, several MC nanocomposite modified electrochemical sensors [36-38] and biosensors [39-41] have been

successfully fabricated to study the oxidation phenomenon of Glu. Though literature reports the utilization of metal oxide (Co_3O_4) supported MCF for catalysis applications [42, 43], it has not been exploited for electrochemical screening of Glu.

In the present work, synthesis of ultra advanced cobalt oxide supported mesoporous carbon framework (Co_3O_4@MCF) has been reported for fabrication of modified GCE biosensor for Glu monitoring (Scheme 1). Chitosan (Chi) has been used as binder to hold Co_3O_4@MCF matrix and to maintain the mechanical stability of the electrode. Nanoassembly of Co_3O_4@MCF-Chi provided a suitable microenvironment and sufficiently large accessible area for the effective immobilization of GOx at GCE electrode. The present study reports excellent biosensing performance of newly designed Co_3O_4@MCF-Chi-GOx/GCE biosensor for Glu detection using electrochemical methods.

Scheme 1

2. Experimental

2.1 Reagents and Chemicals

Polymer precursors 2, 4-dihydroxybenzoic acid, ethylenediamine and hexamethylentetramine (HMT) along with cobalt nitrate, surfactant Pluronic P123, chitosan, GOx and Glu were purchased from Sigma Aldrich (Shanghai, China). The supporting electrolyte 0.1 M phosphate buffer (pH 7.0) was prepared from sodium dihydrogen phosphate and disodium hydrogen phosphate. All other chemical used are of analytical reagent grade.

2.2 Apparatus

All the electrochemical measurements were carried out at electrochemical workstation CHI 440B, (Chenhua Instruments, China). Electrochemical impedance spectroscopic (EIS) measurements were recorded at Metrohm Autolab PGSTAT302N Potentiostat/Galvanostat (Eco

Chemie, The Netherlands). Co_3O_4-MCF-Chi-GOx modified GCE electrode was employed as working electrode while Ag/AgCl (3.0 M KCl) and Pt wire were utilized as reference and as counter electrode respectively. Scanning electron microscopic images (SEM) of prepared nanomaterials were recorded at JEOL JSM-7800F instrument. Transmission electron microscopic (TEM) studies were carried out at JEM-2000EX (JEOL, Japan). HRTEM and energy dispersive x-ray analysis (EDAX) were performed at JEOL JEM-2100. Raman spectra were recorded at Renishaw inVia raman microscope with 532 nm laser excited. X-ray diffraction (XRD) measurements were performed on a Rigaku D/max-2400 diffractometer using Cu-K radiation as X-ray source. The nitrogen sorption experiments were performed at 77 K on a Quantochrome Auto Sorb-1-MP to assess specific surface area and the pore size distribution using Brunauer Emmett Teller (BET) method.

2.3 Synthesis procedure

2.3.1 Preparation of mesoporous carbon framework (MCF)

In a typical synthesis procedure, 3.08 g of 2,4-dihydroxybenzoic acid, 0.6 g of ethylenediamine, 0.934 g of HMT and 3.5 g of Pluronic P123 were dissolved in 80 mL of distilled water. The solution was transferred into a teflon-lined stainless steel autoclave of 120 mL capacity which was tightly sealed and heated up to 130°C for 4 h. The resultant polymer gel was mashed, washed three times with distilled water and dried at 50°C over night. The polymer gel was then carbonized by heating up to 800°C at a heating rate of 2°C min^{-1} for 3h under argon atmosphere. The final material was obtained as mesoporous carbon frameworks (MCF) [43].

2.3.2 Preparation of Co_3O_4@MCF nanocomposite

As prepared polymer product (2 g) was re-dispersed in 43 mL of mixed solution of 34 mL of H_2O and 9 mL of ammonium hydroxide solution (30.0%) containing $Co(NO_3)_2 \cdot 6H_2O$ (0.466 g).

The solution was mixed well and stirred at 50°C for 6 h. The product was then filtered followed by washing with deionized water (3 times) and dried at 50°C under vacuum for 8 h. Finally, Co_3O_4@MCF was obtained by pyrolysis at 500°C with a heating rate of 2°C min^{-1} for 2 h under N_2 treatment. Afterwards, the sample was allowed to cool down to room temperature under N_2 atmosphere.

3. Results and discussion

3.1 Structural characterization

Synthesized Co_3O_4@MCF was structurally and chemically characterized by various microscopic and spectroscopic techniques. Figure 1A and 1B illustrates the typical TEM images of mesoporous Co_3O_4@MCF with an average particle size of 2.96 nm (inset Figure 1B). TEM of pure MCF has been provided in Figure S1. Figure 1C and 1D show the HRTEM images of finely dispersed Co_3O_4 nanoparticles on MCF surface which clearly manifest the successful preparation of Co_3O_4@MCF nanocomposite. In the HRTEM image (Figure 1E), the lattice fringes with d spacing value of 0.24 nm was observed which corresponded to the (311) plane of Co_3O_4. The observation was found in agreement with the SAED pattern (inset Figure 1E) and XRD results. Figure 1F displays SEM image of Co_3O_4@MCF showing 3D gel structure of MCF [43].

Figure 1

Figure 2A exhibites the EDAX pattern of Co_3O_4@MCF. The study demonstrates high proportion of C, O and Co in the prepared Co_3O_4@MCF suggesting successful fabrication of the nanocomposite. The typical raman spectra of Co_3O_4@MCF has been shown by Figure 2B which clearly indicates the characteristic disordered carbon of D band and E2g mode phonons of sp^2 G bands of graphitic carbon at around 1350 cm^{-1} and 1580 cm^{-1} respectively [40]. Further, the specta shows the additional peaks which were related to the vibrational modes of crystalline

Co_3O_4. Raman active modes of Co_3O_4 namely Eg, F_2g^2 and F_2g^1 were confirmed by peaks located around 472 cm^{-1}, 510 cm^{-1}, 611 cm^{-1} respectively. The intense raman peak obtained at 680 cm^{-1} was attributed to the octahedral sites ($Co^{III}O_6$) and was assigned to the to the A_1g mode of the Co_3O_4 crystalline phase [43]. Moreover, Figure 2C represents the obtained XRD pattern of MCF and Co_3O_4@MCF. The prominent peaks of MCF were observed at around 26° and 44° which were related to 002 and 100 plane of MCF [38, 43]. The XRD pattern obtained for Co_3O_4@MCF suggested the presence of prominent 311 plane which is a characteristic of crystalline Co_3O_4 [44, 46-48]. The BET results of the prepared Co_3O_4@MCF have been given in Figure S2 of supporting information showing its mesoporous nature, pore size distribution at around 3 nm and large surface area.

Figure 2

3.2 Fabrication of Co_3O_4@MCF-Chi-GOx/GCE biosensor

For preparation of Co_3O_4@MCF-Chi-GOx modified biosensor, firstly bare GCE was properly washed with ultra pure water and polished with alumina powder of particle size 1.0 µm, 0.3 µm and 0.05 µm on microcloth pads several times. Further, the electrode was sonicated in ethanol/water till a clean mirror like finish was obtained. For the preparation of modified electrode, firstly 10.0 µL of Co_3O_4@MCF solution (3.0 mg mL^{-1}) was thoroughly added to 8.3 µL of water and 15.0 µL of GOx solution (10.0 mg mL^{-1} in 0.1 M PBS). The mixture was sonicated well for 30 min followed by addition of 6.7 µL of chitosan solution (6.0 mg mL^{-1}). A final concentration of 0.75 mg mL^{-1}, 3.6 mg mL^{-1} and 1.0 mg mL^{-1} was calculated for Co_3O_4@MCF, GOx solution and chitosan respectively. A known volume of Co_3O_4@MCF-Chi-GOx suspension (5.0 µL) was drop-casted at pre-cleaned GCE surface and kept at room temperature for drying and used further in electrochemical measurements.

3.3 Electrochemical impedance spectroscopic characterization

The electron transfer resistance (Rct) of developed Co_3O_4@MCF-Chi-GOx/GCE biosensor was evaluated using electrochemical impedance spectroscopy (EIS). The measurements were carried out in 5.0 mM $K_3Fe(CN)_6^{-3/-4}$ containing 0.1M KCl which acted as redox probe. Figure 3A shows the nyquist plots obtained for Co_3O_4@MCF-Chi-GOx/GCE, Chi/GCE, bare GCE and Co_3O_4@MCF-Chi/GCE electrodes. The diameter of the high frequency semicircle in the nyquist plots represents higher value of R_{ct}. Using appropriate equivalent circuit, R_{ct} values were obtained as 2.09 kΩ for Chi/GCE, 917.0 Ω for GCE, 81.7 Ω for Co_3O_4@MCF-Chi-GOx/GCE and 22.4 Ω for Co_3O_4@MCF-Chi/GCE nanosensors. The decreased diameter of the semicircle in the high frequency region of nyquist plot obtained for Co_3O_4@MCF-Chi/GCE was attributed to the increased electron transfer at Co_3O_4@MCF-Chi/GCE. Whereas the little increase in semicircle diameter (R_{ct} value) for Co_3O_4@MCF-Chi-GOx/GCE suggested the successful immobilization of GOx onto Co_3O_4@MCF-Chi film as the enzyme organic matter inhibit the electrical conductivity a little.

3.4 Cyclic voltammetry of fabricated electrodes

Figure 3B indicates cyclic voltammetric (CV) behavior of different fabricated electrodes in nitrogen-saturated 0.1M phosphate buffer (PBS, pH 7.0) at scan rate of 100 mV s^{-1}. The corresponding curves of GOx/GCE (curve black) and Chi-GOx/GCE (curve red) showed no significant redox peaks which revealed their inability to mediate the electron transfer of GOx. However, immobilization of GOx on Co_3O_4@MCF-Chi film resulted in quasi-reversible redox peaks dedicated to conversion of FAD to $FADH_2$. This suggested the efficient immobilization of GOx onto Co_3O_4@MCF-Chi/GCE resulting in greater catalytic activity (curve pink) than Co_3O_4@MCF-Chi/GCE (curve blue).

Figure 3C shows CV of Co_3O_4@MCF-Chi-GOx/GCE in 0.1M phosphate buffer (pH 7.0) at scan rate ranging from 25.0-300.0 mVs^{-1}. The anodic peak current (Ipa) and cathodic peak current (Ipc) were found linearly proportional to the scan rate as shown in Figure 3D which suggested successful electron transfer between GOx enzyme active center and electrode. The corresponding linear regression equations have been given below,

$Ipa = 0.0442\ \upsilon + 2.4922\ (r^2 = 0.9842)$ (1)

$Ipc = -0.0524\ \upsilon + 3.2982\ (r^2 = 0.9940)$ (2)

With increasing scan rate, the oxidation peak was observed with more positive shift while the reduction peak was observed to shift towards more negative values indicating the peak-to-peak separation (Ep) increasing gradually.

Figure 3

4. Electrochemical biosensing application of Co_3O_4@MCF-Chi-GOx/GCE electrode

4.1 Electrocatalytic activity of Co_3O_4@MCF-Chi-GOx/GCE biosensor towards glucose

Figure 4A shows the effect of dissolved oxygen (O_2) on the electrochemical activity of Co_3O_4@MCF-Chi-GOx/GCE biosensor towards Glu sensing. The cyclic voltammetric response of fabricated biosensor in nitrogen-saturated 0.1M PBS (pH 7.0) was evaluated at scan rate of 100 mV s^{-1} (curve blue). In air saturated atmosphere, Co_3O_4@MCF-Chi-GOx/GCE biosensor showed a sharp increase in the cathodic peak current and decrease in the anodic peak current of GOx (curve black) which could be ascribed to the high oxygen reduction reaction (ORR) activity of the fabricated electrode according to reactions (3) and (4) [14, 38];

$GOx\text{-}FAD + 2e^- + 2H^+ \leftrightarrow GOx\text{-}FADH_2$ (3)

$GOx\text{-}FADH_2 + O_2 \rightarrow GOx\text{-}FAD + H_2O_2$ (4)

However, the addition of Glu (1.0 mM) to oxygen saturated PBS led to sudden decrease in the reduction current at Co_3O_4@MCF-Chi-GOx/GCE (curve red). The basic mechanism lied in the fact that the redox response was mainly due to FAD cofactor that was considered to be dissociated from GOx and adsorbed to the electrode (Co_3O_4@MCF-Chi/GCE) surface. The reduction of O_2 occurred generally by the electrode surface. However, addition of Glu resulted in O_2 consumption by GOx and thus less O_2 was reduced by the electrode and peak current was decreased.

GOx catalyzed oxidation of Glu can be written as following reaction (5) [14, 38];

$$\text{Glu} + \text{GOx-FAD} \rightarrow \text{Gluconolactone} + \text{GOx-FADH}_2 \quad (5)$$

The study suggested the potential applicability of developed Co_3O_4@MCF-Chi-GOx/GCE for Glu biosensing applications. Furthermore, cyclic voltammetry of Co_3O_4@MCF-Chi-GOx/GCE was performed in air saturated 0.1M PBS (pH 7.0) at 100 mV s^{-1} with increasing concentrations of Glu upto 1800.0 μM (Figure 4B). It was noticed that the oxidation of Glu by GOx at Co_3O_4@MCF-Chi-GOx/GCE consumed the dissolved oxygen which led to the decrease in reduction peak current.

Figure 4

4.2 Amperometric study of Co_3O_4@MCF-Chi-GOx/GCE towards glucose biosensing

Amperometric response of Co_3O_4@MCF-Chi-GOx/GCE was studied for detection of Glu in the concentration range upto 1700.0 μM. Aliquots of Glu were injected at a regular intervals of 50 s into continuously stirred air saturated PBS (pH 7.0). Rapid and well defined amperometric response was observed after each addition of Glu as shown in Figure 5A. Linear calibration plot between increasing Glu concentrations and oxidation current Ip was drawn (Figure 5B) and shown by the following equation (6);

$Ip\ (\mu A) = 0.0001(\mu M) + 0.401\ (r^2 = 0.9975)$ (6)

The limit of detection (LOD) and quantification (LOQ) for Glu at developed Co_3O_4@MCF-Chi-GOx/GCE were obtained as 107.70 μM and 359.01 μM respectively. The results demonstrate better detection performance of the developed biosensor compared to other enzymatic biosensors and nonenzymatic sensors towards Glu detection as shown in Table 1 [49-55].

Figure 5

4.3 Reproducibility and stability

The reproducibility of the fabricated Co_3O_4@MCF-Chi-GOx/GCE biosensor was investigated using amperometry at different time intervals by eight successive measurements using 1.0 mM Glu. For three individual freshly prepared electrodes, RSD of 4.70 % was obtained under similar experimental conditions which demonstrated an acceptable reproducibility of the biosensor towards Glu analysis. The stability of Co_3O_4@MCF-Chi-GOx/GCE electrode was examined by measuring the current-time response towards Glu oxidation after four weeks of storage at 4ºC. The biosensor showed 88% of initial current response demonstrating a long term stability of the electrode for electrochemical measurements. Better stability of biosensor could be attributed to the good biocompatibility of Co_3O_4@MCF-Chi matrix which offered a suitable microenvironment for GOx to retain its bioactivity.

4.4 Interference studies and real sample analysis

Figure 6 shows the excellent selectivity and anti-interference ability of Co_3O_4@MCF-Chi-GOx/GCE towards Glu detection. The selectivity of the sensor was evaluated by amperometry adding interfering moties. The current-time curve of Glu remained unaffected in presence of various interfering substances. No significant change in current response was observed on addition of ascorbic acid (AA), dopamine (DA), uric acid (UA) and fructose suggesting high

selectivity of the developed bisensor for Glu detection. The developed biosensor was successfully applied for the detection of glucose in blood serum samples without any extraction step but dilution only. The amount of glucose present in blood serum found to be 3.62 mM which was further confirmed by standard colorimetric method demonstrating good accuracy for glucose screening in real samples.

Figure 6

5. Conclusion

In summary, advanced functional nanostructures based on Co_3O_4 supported mesoporous carbon frameworks were synthesized using simple hydrothermal and pyrolysis method. The prepared Co_3O_4@MCF nanocomposite was chemically characterized and exploited for electrochemical biosensing of Glu. Structural and spectroscopic examination confirmed the successful preparation of Co_3O_4@MCF and presence of finely dispersed crystalline Co_3O_4 on the mesoporous carbon framework. Co_3O_4@MCF exhibited better electrical conductivity, large surface area and high porosity which allowed efficient immobilization of GOx onto its surface for facilitated electron transfer towards electrochemical determination of Glu. Addition of Glu to the air saturated PBS medium resulted in O_2 consumption by GOx and led to decreased electrochemical signal. With, good reproducibility, stability and excellent anti-interference ability, the developed Co_3O_4@MCF-Chi-GOx/GCE biosensor can be applied for routine analysis of glucose in different real samples. Moreover, the biosensor holds great promise for its effective implications in point-of-care diagnostic devices.

Acknowledgements

ACCEPTED MANUSCRIPT

This work was supported by the Chinese Academy of Sciences through President's International Fellowship Initiative for Postdoctoral Researcher Dhanjai (2015PM002), by National Natural Science Foundation of China (21577139).

Note: Authors declare no competing interests

ACCEPTED MANUSCRIPT

6. References

[1]. M. Labib, E.H. Sargent, S.O. Kelley, Electrochemical methods for the analysis of clinically relevant biomolecules, Chemical Reviews, 116 (2016) 9001-9090.

[2]. Dhanjai, A. Sinha, L. Wu, X. Lu, D. Tan, J. Chen, Voltammetric Sensing of Biomolecules at Carbon Based Electrode Interfaces: A Review, TRAC-Trend. Anal. Chem., 98 (2018) 174-189.

[3]. Dhanjai, A. Sinha, Amperometric response characteristics of rabeprazole at N-doped MWCNTs-chitosan nanosensor in solubilized system, J Electrochem. Soc., 164 (9) (2017) H639-H646.

[4]. Dhanjai, A. Sinha, L. Wu, X. Lu, J. Chen, Advances in Sensing and Biosensing of Bisphenols: A Review, Anal. Chim. Acta, 998 (2018) 1-27.

[5]. C. Chen, Q. Xie, D. Yang, H. Xiao, Y. Fu, Y. Tan, S. Yao, Recent advances in electrochemical glucose biosensors: a review, RSC Advances, 3 (2013) 4473-4491.

[6]. L. Zhao, G. Wu, Z. Cai, T. Zhao, Q. Yao, X. Chen, Ultrasensitive non-enzymatic glucose sensing at near-neutral pH values via anodic stripping voltammetry using a glassy carbon electrode modified with Pt_3Pd nanoparticles and reduced graphene oxide, Microchim. Acta, 182 (2015) 2055-2060.

[7]. Z. Li, L. Sheng, A. Meng, C. Xie, K. Zhao, A glassy carbon electrode modified with a composite consisting of reduced graphene oxide, zinc oxide and silver nanoparticles in a chitosan matrix for studying the direct electron transfer of glucose oxidase and for enzymatic sensing of glucose, Microchim. Acta, 183 (2016) 1625-1632.

[8]. S. Aslan, U. Anik, Microbial glucose biosensors based on glassy carbon paste electrodes modified with Gluconobacter Oxydans and graphene oxide or graphene-platinum hybrid nanoparticles, Microchim. Acta, 183 (2016) 73-81.

[9]. C. Ye, X. Zhong, Y. Chai, R. Yuan, Sensing glucose based on its affinity for concanavalin A on a glassy carbon electrode modified with a C_{60} fullerene nanocomposite, Microchim. Acta, 182 (2015) 2215-2221.

[10]. P. Das, M. Das, S.R. Chinnadayyala, I.M. Singha, P. Goswami, Recent advances on developing 3rd generation enzyme electrode for biosensor applications, Biosens. Bioelectron., 79 (2016) 386–397.

[11]. Y. Wang, H. Li, J. Kong, Facile preparation of mesocellular graphene foam for direct glucose oxidase electrochemistry and sensitive glucose sensing, Sens. Actuators B, 193 (2014) 708– 714.

[12]. V. Mani, B. Devadas, S.M. Chen, Direct electrochemistry of glucose oxidase at electrochemically reduced graphene oxide-multiwalled carbon nanotubes hybrid material modified electrode for glucose biosensor, Biosens. Bioelectron., 41 (2013) 309–315.

[13]. B. Thirumalraj, S. Palanisamy, S.M. Chen, C.Y. Yang, P. Periakaruppan, B.S. Lou, Direct electrochemistry of glucose oxidase and sensing of glucose at a glassy carbon electrode modified with a reduced graphene oxide/fullerene-C_{60} composite, RSC Advances, 5 (2015) 77651–77657.

[14]. R. Devasenathipathy, V. Mani, S.M. Chen, S.T. Huang, T.T. Huang, C.M. Lin, K.Y. Hwa, T.Y. Chen, B.J. Chen, Glucose biosensor based on glucose oxidase immobilized at gold nanoparticles decorated graphene-carbon nanotubes, Enzyme Microb. Technol., 78 (2015) 40–45.

[15]. S. Palanisamy, C. Karuppiah, S.M. Chen, Direct electrochemistry and electrocatalysis of glucose oxidase immobilized on reduced graphene oxide and silver nanoparticles nanocomposite modified electrode, Colloid Surf. B: Biointerfaces, 114 (2014) 164– 169.

[16]. L. Chen, H. Xie, J. Li, Electrochemical glucose biosensor based on silver nanoparticles/multiwalled carbon nanotubes modified electrode, J Solid State Electrochemistry, 16 (2012) 3323–3329.

[17]. Q. Xu, S.X. Gu, L. Jin, Y. Zhou, Z. Yang, W. Wang, X. Hu, Graphene/polyaniline/gold nanoparticles nanocomposite for the direct electron transfer of glucose oxidase and glucose biosensing, Sens. Actuators B, 190 (2014) 562– 569.

[18]. X. Feng, H. Cheng, Y. Pan, H. Zheng, Development of glucose biosensors based on nanostructured graphene-conducting polyaniline composite, Biosens. Bioelectron., 70 (2015) 411–417.

[19]. J. Li, Z. Yang, Y. Tang, Y. Zhang, X. Hu, Carbon nanotubes-nanoflake-like SnS_2 nanocomposite for direct electrochemistry of glucose oxidase and glucose sensing, Biosens. Bioelectron., 41 (2013) 698–703.

[20]. Y. Yu, Z. Chen, S. He, B. Zhang, X. Li, M. Yao, Direct electron transfer of glucose oxidase and biosensing for glucose based on PDDA-capped gold nanoparticle modified graphene/multiwalled carbon nanotubes electrode, Biosens. Bioelectron., 52 (2014) 147–152.

[21]. S. Wang, L.P. Xu, H.W. Liang, S.H. Yu, Y. Wen, S. Wang, X. Zhang, Self-interconnecting Pt nanowire network electrode for electrochemical amperometric biosensor, Nanoscale, 7 (2015) 11460-11467.

[22]. J.Y. Park, Y.H. Kim, A. Seong, Y.J. Yoo, amperometric determination of glucose based on the direct electron transfer between glucose oxidase and tin oxide, Biotechnol. Bioprocess Eng., 13 (2008) 431-435.

[23]. H. N. Choi, M.A. Kim, W.Y. Lee, Amperometric glucose biosensor based on sol–gel-derived metal oxide/Nafion composite films, Anal. Chim. Acta, 537 (2005) 179–187.

[24]. J. Li, Y. Tang, J. Yang, Z. Yang, Y. Zhang, X. Hu, Cage-like PbS nanostructure for the construction of novel glucose electrochemical biosensor, Sens. Actuators B, 190 (2014) 549–554.

[25]. P.A. Palod, V. Singh, Improvement in glucose biosensing response of electrochemically grown polypyrrole nanotubes by incorporating crosslinked glucose oxidase, Mat. Sci. Eng. C, 55 (2015) 420–430.

[26]. Q. Zhang, S. Wu, L. Zhang, J. Lu, F. Verproot, y. Liu, Z. Xing, J. Li, X. M. Song, Fabrication of polymeric ionic liquid/graphene nanocomposite for glucose oxidase immobilization and direct electrochemistry, Biosens. Bioelectron., 26 (2011) 2632–2637.

[27]. F. Mehrabi, A. Vafaei, M. Ghaedi, A.M. Ghaedi, E.A. Dil, A. Asfaram, Ultrasound assisted extraction of Maxilon Red GRL dye from water samples using cobalt ferrite nanoparticles loaded on activated carbon as sorbent: Optimization and modeling, Ultrasonics sonochemistry, 38 (2017) 672-680.

[28]. E.A. Dil, M. Ghaedi, A. Asfaram, F. Zare, F. Mehrabi, F. Sadeghfar, Comparison between dispersive solid-phase and dispersive liquid-liquid microextraction combined with spectrophotometric determination of malachite green in water samples based on ultrasound-assisted and preconcentration under multi-variable experimental design optimization, Ultrasonics sonochemistry, 39 (2017) 374-383.

[29]. E.A. Dil, M. Ghaedi, A. Asfaram, F. Mehrabi, A.A. Bazrafshan, Optimization of process parameters for determination of trace Hazardous dyes from industrial wastewaters based on nanostructures materials under ultrasound energy, Ultrasonics sonochemistry, 40 (2018) 238-248.

[30]. E.A. Dil, M. Ghaedi, A. Asfaram, Optimization and modeling of preconcentration and determination of dyes based on ultrasound assisted-dispersive liquid-liquid microextraction coupled with derivative spectrophotometry, Ultrasonics sonochemistry, 34 (2017) 27-36.

[31]. E.A. Dil, M. Ghaedi, A. Asfaram, A. Goudarzi, Synthesis and characterization of ZnO-nanorods loaded onto activated carbon and its application for efficient solid phase extraction and determination of BG from water samples by micro-volume spectrophotometry, New Journal of Chemistry, 39 (2015) 9407-9414.

[32]. A. Walcarius, Recent trends on electrochemical sensors based on ordered mesoporous carbon, Sensors, 17 (2017) 1863.

[33]. T. Wang, Z. Peng, Y. Wang, J. Tang, G. Zheng, MnO nanoparticle@mesoporous carbon composites grown on conducting substrates featuring high-performance lithium-ion battery, supercapacitor and sensor, Sci. Rep., 3 (2013) 2693.

[34]. J.C. Ndamanisha, L. Guo, Nonenzymatic glucose detection at ordered mesoporous carbon modified electrode, Bioelectrochemistry, 77 (2009) 60–63.

[35]. E. Ghasemi, E. Shams, N.F. Nejad, Covalent modification of ordered mesoporous carbon with glucose oxidase for fabrication of glucose biosensor, J Electroanal. Chem., 752 (2015) 60–67.

[36]. C. Su, C. Zhang, G. Lu, C. Ma, Nonenzymatic electrochemical glucose sensor based on pt nanoparticles/mesoporous carbon matrix, Electroanalysis, 22 (2010) 1901 – 1905.

[37]. P. Qi, S. Chen, J. Chen, J. Zheng, X. Zheng, Y. Yuan, Catalysis and reactivation of ordered mesoporous carbon-supported gold nanoparticles for the base-free oxidation of glucose to gluconic acid, ACS Catalysis, 5 (2015) 2659−2670.

[38]. L. Wang, J. Bai, X. Bo, X. Zhang, L. Guo, A novel glucose sensor based on ordered mesoporous carbon–Au nanoparticles nanocomposites, Talanta, 83 (2011) 1386–1391.

[39]. F. Teng, X. Wang, C. Shen, S. Li, A micro glucose sensor based on direct prototyping mesoporous carbon electrode, Microsyst. Technol., 21 (2015) 1337–1343.

[40]. D. Xiang, L. Yin, J. Ma, E. Guo, Q. Li, Z. Li, K. Liu, Amperometric hydrogen peroxide and glucose biosensor based on $NiFe_2$/ordered mesoporous carbon nanocomposites, Analyst, 140 (2015) 644-653.

[41]. J. Chen, R. Zhu, J. Huang, M. Zhang, H. Liu, M. Sun, L. Wang, Y. Song, A glucose biosensor based on glucose oxidase immobilized on three-dimensional porous carbon electrodes, Analyst, 140 (2015) 5578-5584.

[42]. S. Dou, X. Li, L. Tao, J. Huo, S. Wang, Cobalt nanoparticle-embedded carbon nanotube/porous carbon hybrid derived from MOF-encapsulated Co3O4 for oxygen electrocatalysis, Chem. Commun., 52 (2016) 9727-9730.

[43]. G.H. Wang, X. Deng, D. Gu, K. Chen, H. Tuysuz, B. Spliethoff, H.J. Bongard, C. Weidenthaler, W. Schmidt, F. Schuth, Co_3O_4 nanoparticles supported on mesoporous carbon for selective transfer hydrogenation of αβ-unsaturated aldehydes, Angew. Chem. Int. Ed., 55 (2016) 11101-11105.

[44]. C. Sengottaiyan, R. Jayavel, P. Bairi, R.G. Shrestha, K. Ariga, L.K. Shrestha, Cobalt oxide/reduced graphene oxide composite with enhanced electrochemical supercapacitance performance, Bull. Chem. Soc. Japan, 90 (2017) 955–962.

[45]. C.W. Tang, C.B. Wang, S.H. Chien, Characterization of cobalt oxides studied by FT-IR, Raman, TPR and TG-MS, Thermochim. Acta, 473 (2008) 68–73.

[46]. Y. Wang, D. Cao, X. Zhao, Heterogeneous degradation of refractory pollutants by peroxymonosulfate activated by CoOx-doped ordered mesoporous carbon, Chem. Engineer. Journal, 328 (2017) 1112–1121.

[47]. T.N. Pham, T. Sharifi, R. Sandström, W. Siljebo, A. Shchukarev, K. Kordas, T. Wågberg, J.P. Mikkola, Robust hierarchical 3D carbon foam electrode for efficient water electrolysis, Sci. Rep., 7 (2017) 6112.

[48]. A.M. Cao, J.S. Hu, H.P. Liang, W.G Song, L.J. Wan, X.L. He, X.G. Gao, S.H. Xia, Hierarchically structured cobalt oxide (Co_3O_4): the morphology control and its potential in sensors, J. Phys. Chem. B, 110 (2006) , 15858-15863.

[49]. K. Wang, Q. Liu, Q.M. Guan, J. Wu, H.N. Li, J.J. Yan, Enhanced direct electrochemistry of glucose oxidase and biosensing for glucose via synergy effect of graphene and CdS nanocrystals, Biosen. Bioelectron., 26 (2011) 2252-2257.

[50]. C. Shan, H. Yang, D. Han, Q. Zhang, A. Ivaska, L. Niu, Graphene/AuNPs/chitosan nanocomposites film for glucose biosensing, Biosen. Bioelectron., 25 (2010) 1070-1074.

[51]. Yi.Wang, H. Li, J. Kong, Facile preparation of mesocellular graphene foam for direct glucose oxidase electrochemistry and sensitive glucose sensing, Sens. Actuators B, 193 (2014) 708-714.

[52]. H. Zhang, Z. Meng, Q.Wang, J. Zheng, A novel glucose biosensor based on direct electrochemistry of glucose oxidase incorporated in biomediated gold nanoparticles–carbon nanotubes composite film, Sens. Actuators B, 158 (2011) 23-27.

[53]. S. Palanisamy, C. Karuppiah, S.M. Chen, Direct electrochemistry and electrocatalysis of glucose oxidase immobilized on reduced graphene oxide and silver nanoparticles nanocomposite modified electrode, Colloids Surf. B, 114 (2014) 164-169.

[54]. Y. Liu, S. Wu, H. Ju, L. Xu, Amperometric glucose biosensing of gold nanoparticles and carbon nanotube multilayer membranes, Electroanalysis, 19 (2007) 986-992.

[55]. M.H. Yang, B.G. Choi, H.S. Park, W.H. Hong, S.Y. Lee, T.J. Park, Development of a glucose biosensor using advanced electrode modified by nanohybrid composing chemically modified graphene and ionic liquid, Electroanalysis, 22 (2010) 1223-1228.

ACCEPTED MANUSCRIPT

Table 1. Comparison of developed Co_3O_4@MCF-Chi-GOx/GCE biosensor perfomance with other glucose sensors and biosensors

Sensor/Biosensor	Limit of Detection (LOD)	Ref.
GOx/Graphene-CDs	700 µM	49
Graphene/AuNPs/chitosan	180 µM	50
Gox-MGF	250 µM	51
AuNPs–GOx–MWCNTs–PVA/GCE	200 µM	52
RGO/Ag/GOx	160 µM	53
AuNPs/ MWCNTs/Gox	128 µM	54
GOx/CMG-IL/Au	376 µM	55
Co_3O_4@MCF-Chi-GOx/GCE	107.7 µM	This Work

Abreviations: CDs-Cadmium sulfide nanocrystals; AuNPs-Gold nanoparticles; MGF-Mesocellular graphene foam; MWCNTs-Multiwalled carbon nanotubes; PVA-Polyvinyl alcohol; RGO-Reduced graphene; CMG-Chemically modified graphene; IL-Ionic liquids.

ACCEPTED MANUSCRIPT

Figures captions:

Scheme 1: (A) Preparation of Co_3O_4@MCF-Chi-GOx/GCE electrode (B) Glucose oxidation reaction catalyzed by GOx at prepared interface.

Figure 1: (A-B) TEM images of Co_3O_4@MCF**,** (C-D) HRTEM images of finely dispersed Co_3O_4 at MCF surface, (E) HRTEM image of Co_3O_4@MCF showing lattice fringe; inset: SAED pattern (F) SEM image of Co_3O_4@MCF.

Figure 2: (A) EDAX, (B) raman spectra and (C) XRD pattern of Co_3O_4@MCF.

Figure 3: (A) Nyquist plots obtained at different electrodes in 5.0 mM $[Fe(CN)6]^{3-/4-}$ containing 0.1 M KCl; (B) CV of different electrodes in nitrogen saturated atmosphere 0.1 M phosphate buffer (pH 7.0) at scan rate 100 mV s^{-1}; (C) cyclic voltammograms of Co_3O_4@MCF-Chi-GOx/GCE in 0.1 M phosphate buffer (pH 7.0) at scan rate between 25.0-300.0 mV s^{-1}; (D) corresponding plots of Ipc and Ipa Vs scan rate in forward and reverse scan.

Figure 4: (A) CV of Co_3O_4@MCF-Chi-GOx/GCE in 0.1 M phosphate buffer (pH 7.0) at scan rate 100 mV s^{-1} in N_2 and air saturated atmosphere; (B) CV of Co_3O_4@MCF-Chi-GOx/GCE at 100 mV s^{-1} for addition of glucose concentrations upto 1800.0 μM.

Figure 5: (A) Current-time response curves of Co_3O_4@MCF-Chi-GOx/GCE for successive addition of glucose into a stirring solution of PBS (pH 7.0) in air saturated atmosphere; (B) corresponding linear calibration plot for glucose concentrations upto 1700.0 μM.

Figure 6: Current-time response curves of Co_3O_4@MCF-Chi-GOx/GCE biosensor for glucose detection in presence of potential interferences, such as uric acid, ascorbic acid, dopamine and fructose.

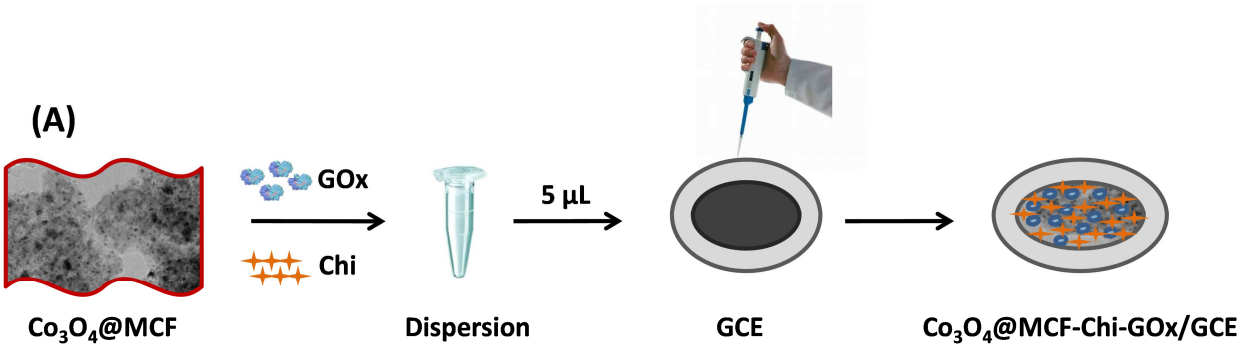

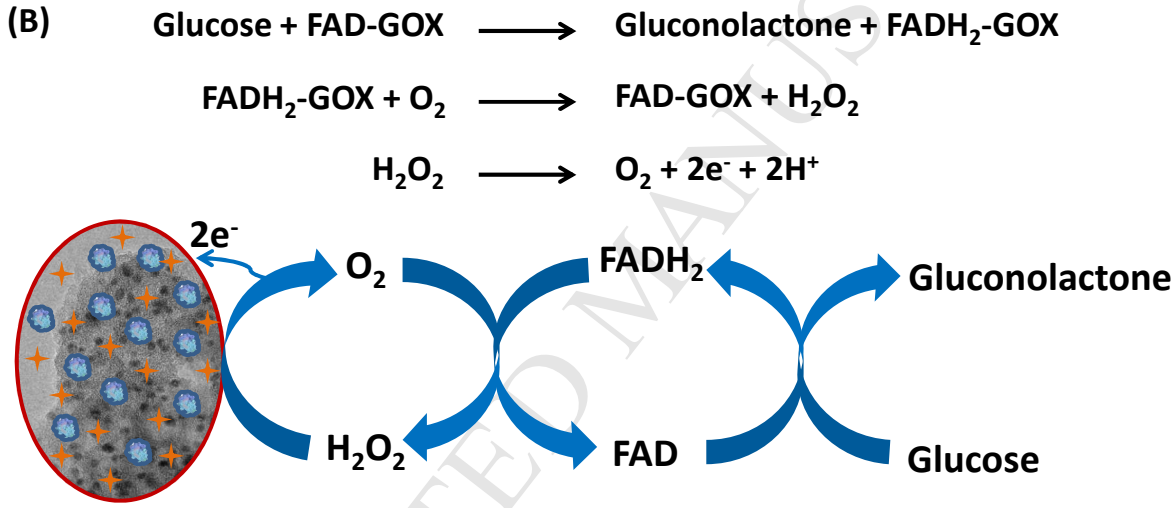

Scheme 1

ACCEPTED MANUSCRIPT

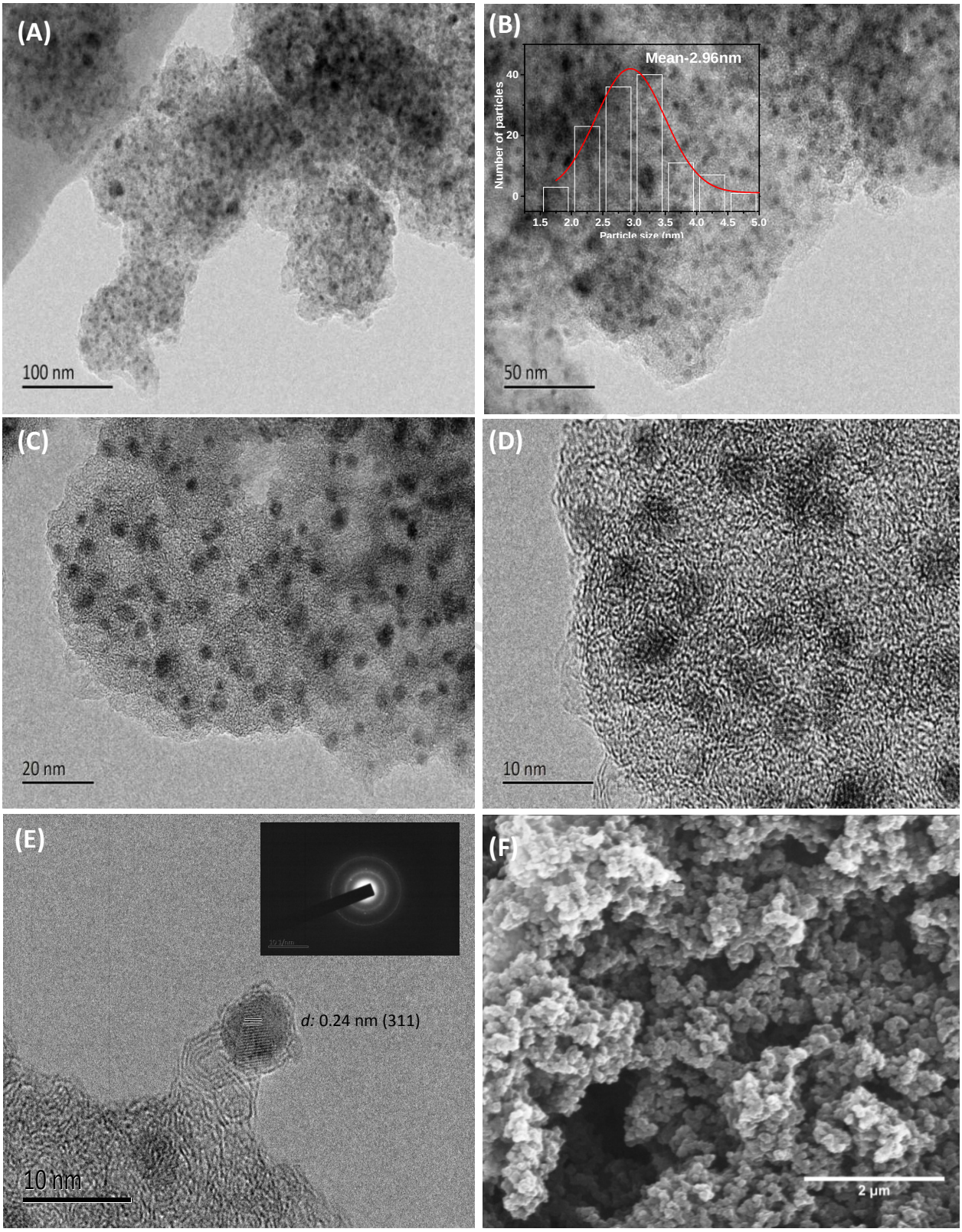
(A)
100 nm
(B)
Mean-2.96nm
Number of particles
40
20
0
1.5
2.0
2.5
3.0
3.5
4.0
4.5
5.0
Particle size (nm)
50 nm
(C)
20 nm
(D)
10 nm
(E)
d: 0.24 nm (311)
10 nm
(F)
2 µm

Figure 1

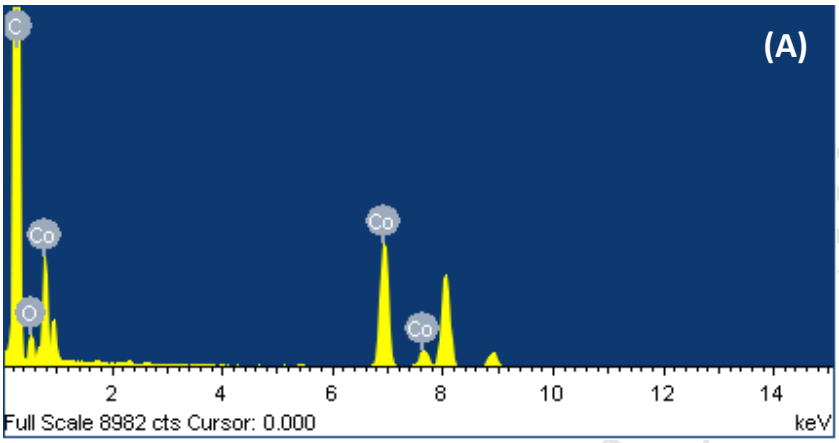

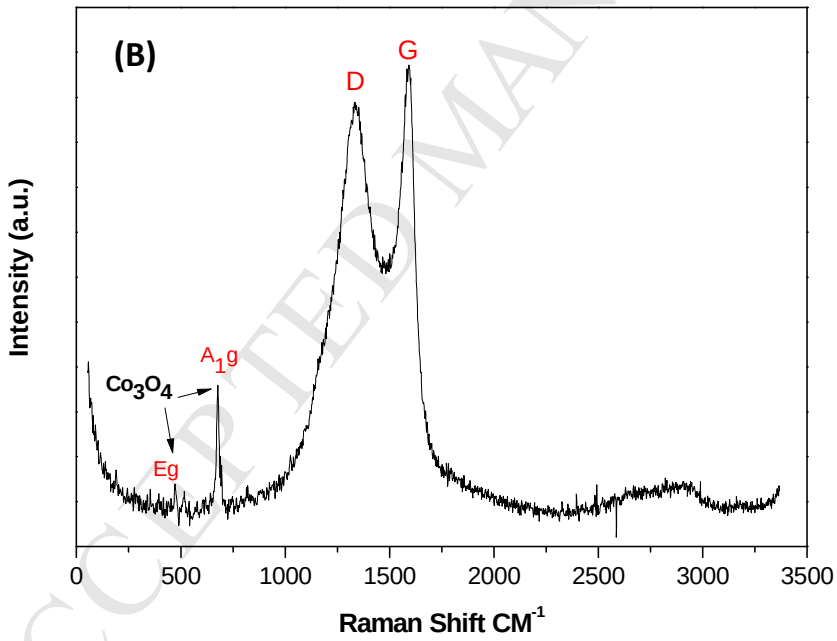

ACCEPTED MANUSCRIPT

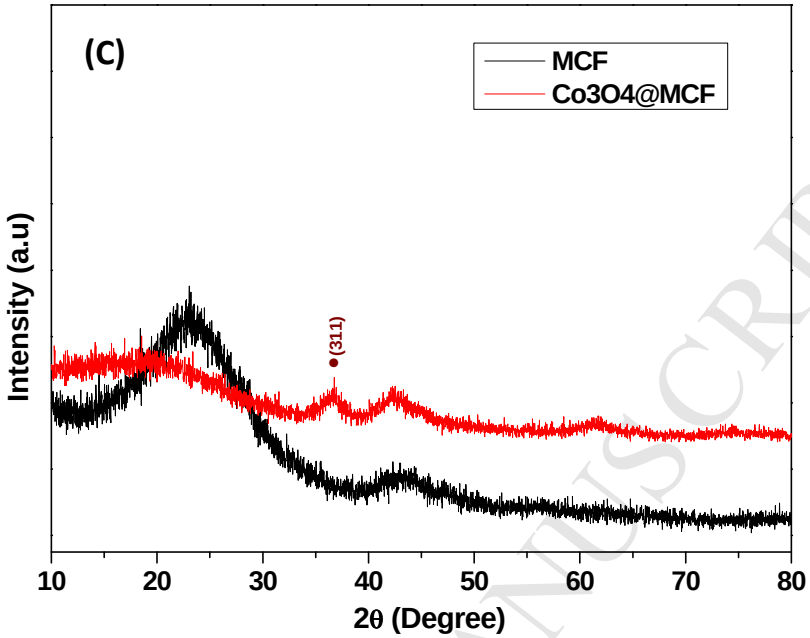

Figure 2

ACCEPTED MANUSCRIPT

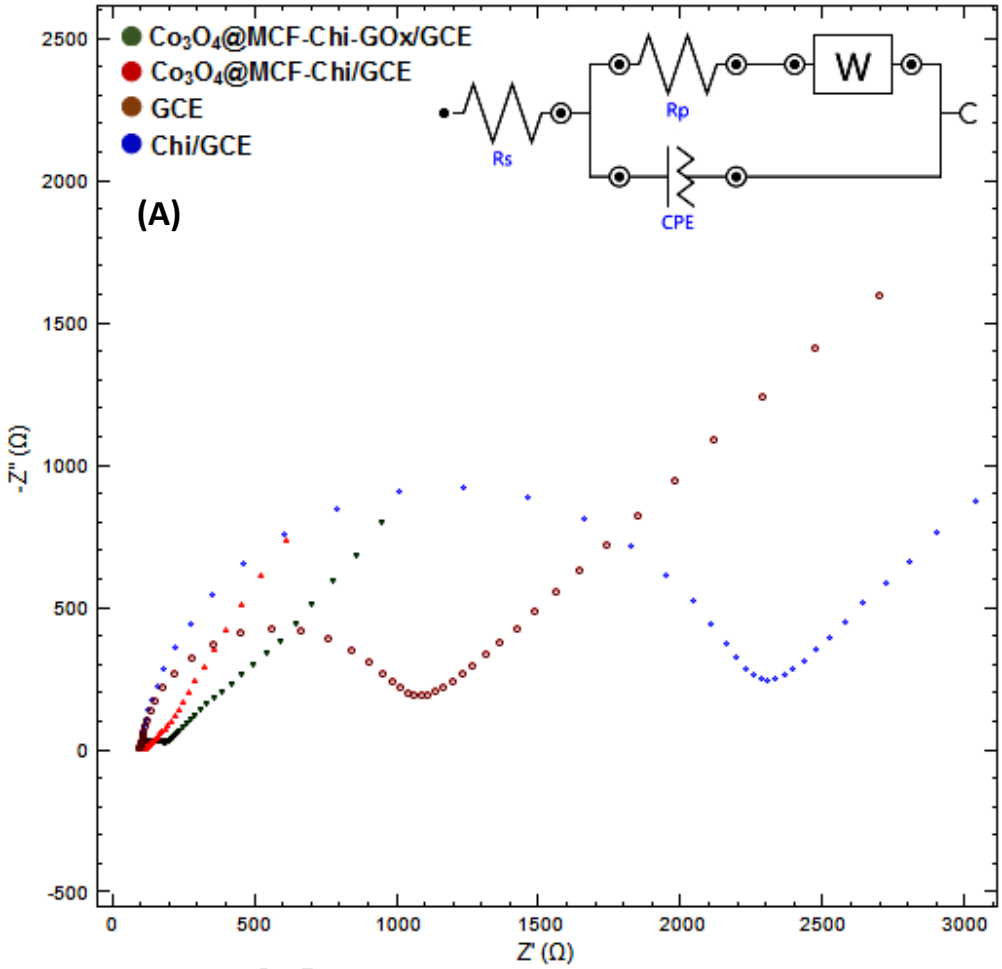
Co3O4@MCF-Chi-GOx/GCE
Co3O4@MCF-Chi/GCE
GCE
Chi/GCE
(A)
Rs
Rp
W
C
CPE
-Z'' (Ω)
Z' (Ω)
2500
2000
1500
1000
500
0
-500
0
500
1000
1500
2000
2500
3000

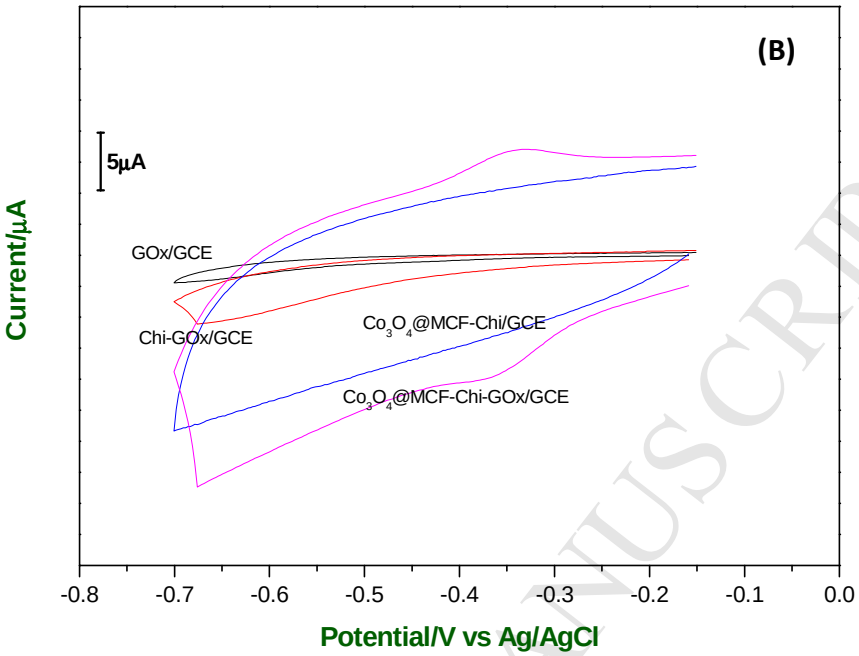

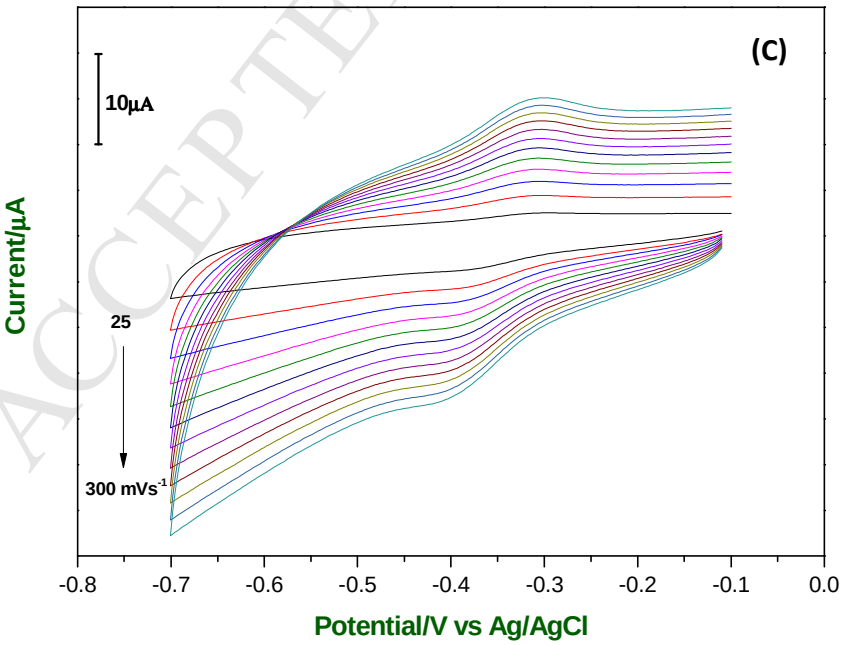

ACCEPTED MANUSCRIPT

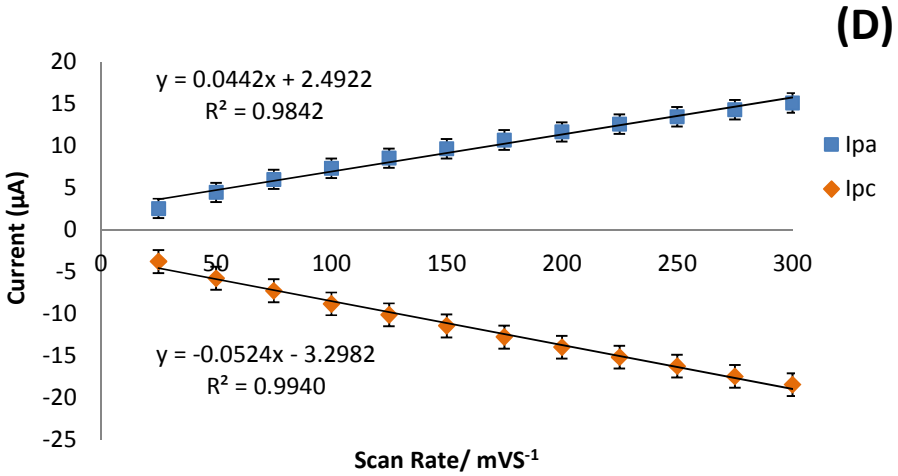

Figure 3

ACCEPTED MANUSCRIPT

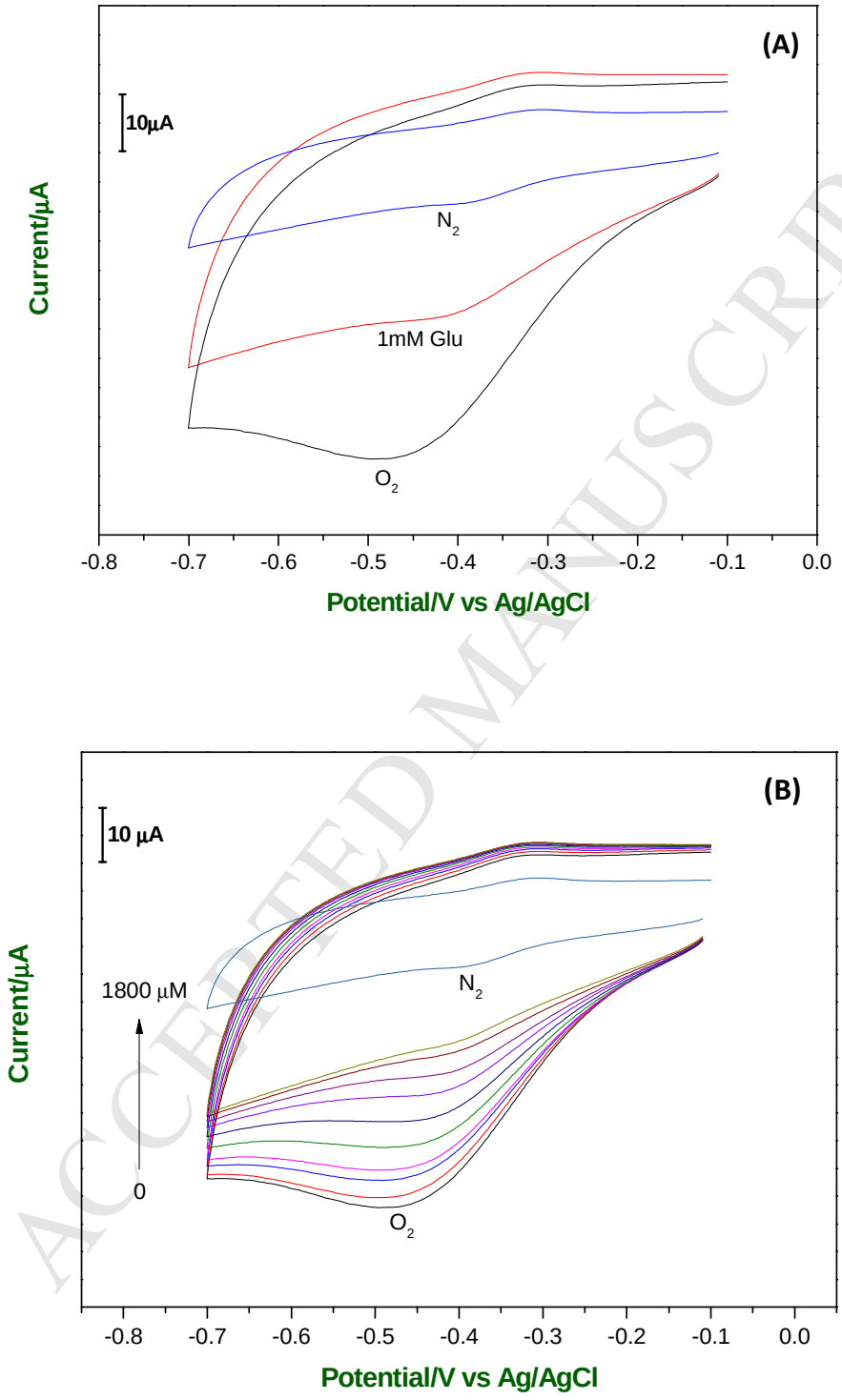
(A)
10μA
N2
1mM Glu
O2
Current/μA
-0.8
-0.7
-0.6
-0.5
-0.4
-0.3
-0.2
-0.1
0.0
Potential/V vs Ag/AgCl
(B)
10 μA
1800 μM
0
N2
O2
Current/μA
-0.8
-0.7
-0.6
-0.5
-0.4
-0.3
-0.2
-0.1
0.0
Potential/V vs Ag/AgCl

Figure 4

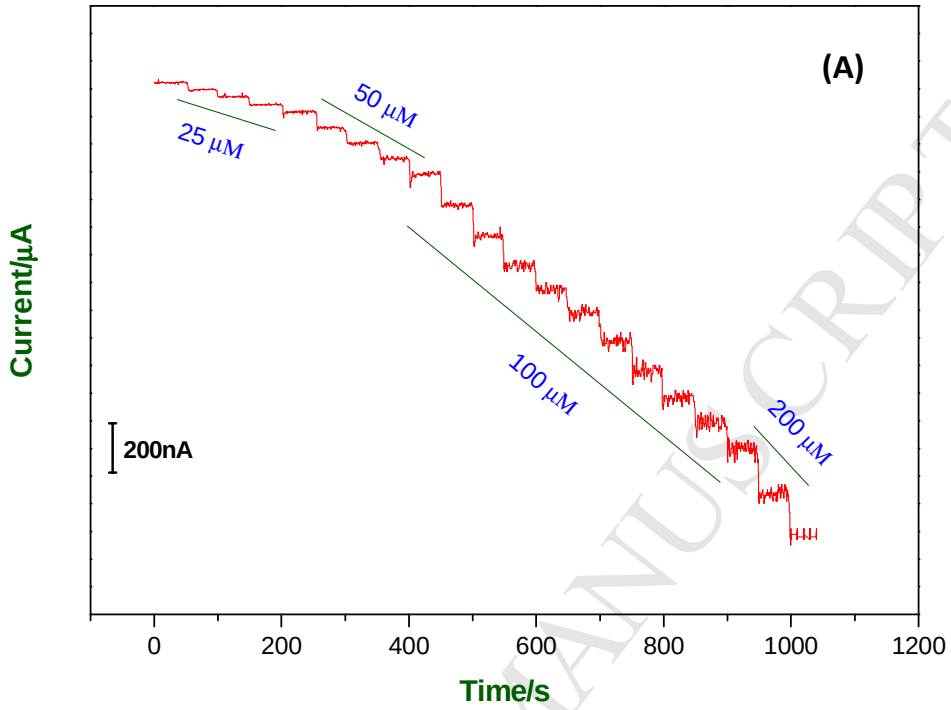

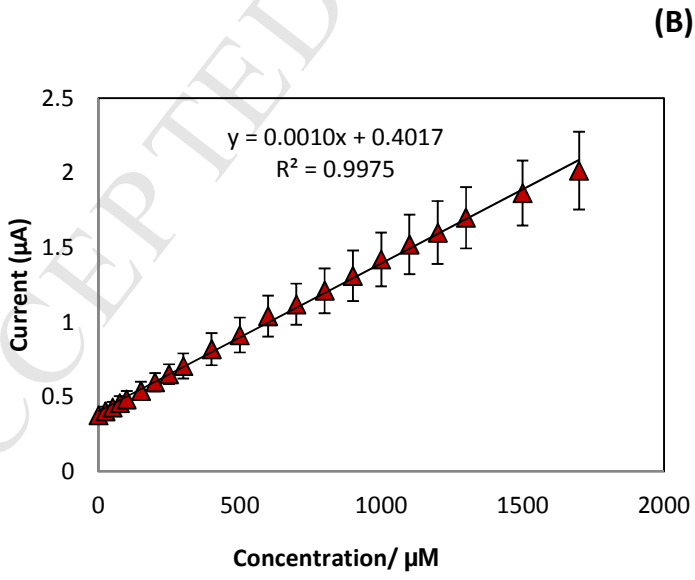

Figure 5

ACCEPTED MANUSCRIPT

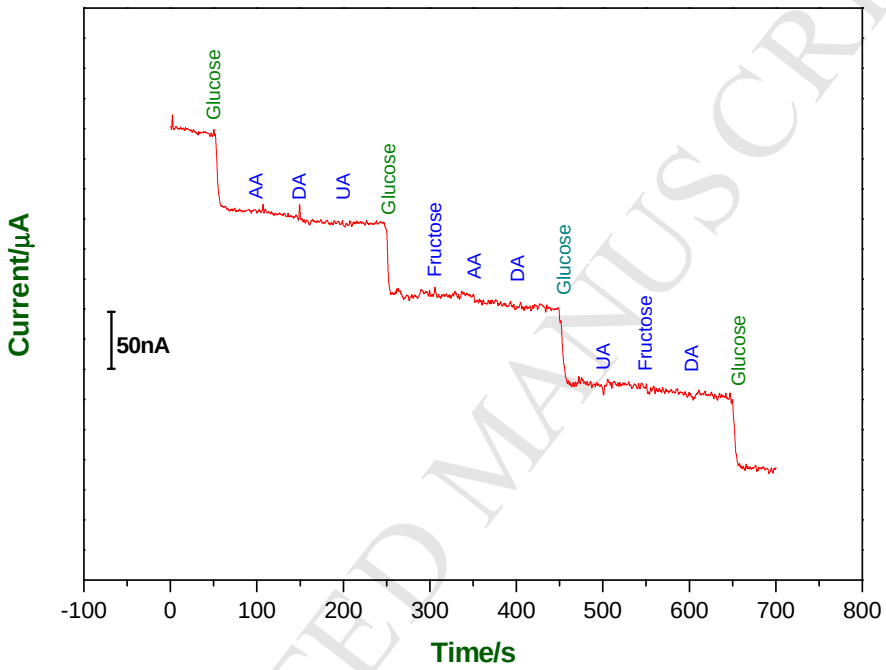

Figure 6

ACCEPTED MANUSCRIPT

ACCEPTED MANUSCRIPT

Highlights

- Co_3O_4 nanoparticles integrated mesoporous carbon framework (Co_3O_4/MCF) has been successfully synthesized using simple hydrothermal, pyrolysis and carbonization reactions.
- Enzymatic biosensing interface was fabricated by immobilizing glucose oxidase (GOx) at Co_3O_4/MCF matrix.
- Glucose was used as model target to exploit the electrochemical performance of Co_3O_4/MCF/GOx biosensing interface using voltammetry and amperometry.
- Biosensor based on Co_3O_4/MCF matrix exhibited high sensitivity and selectivity for glucose than fructose, dopamine, ascorbic acid and uric acid.

ACCEPTED MANUSCRIPT